XAFS Study of the Al K-Edge in $NaAlH_4$

Cornelis P. Baldé,[†] Ana E. Mijovilovich,[†] Diederik C. Koningsberger,[†] Ad M. J. van der Eerden,[†] Andy D. Smith,[‡] Krijn P. de Jong,[†] and Johannes H. Bitter*[,†]

Inorganic Chemistry and Catalysis, Department of Chemistry, Faculty of Science, Universiteit Utrecht, Sorbonnelaan 16, 3584 CA Utrecht, The Netherlands, and CCLRC Daresbury Laboratory, Keckwick Lane, Daresbury, Warrington, Cheshire WA4 4AD, United Kingdom

Received: December 18, 2006; In Final Form: May 23, 2007

Al K-edge (1561.1 eV) XANES and EXAFS spectra of unoxidized $NaAlH_4$, a hydrogen storage material, have been recorded in He atmosphere in a special in situ low-energy cell. The XANES spectrum of $NaAlH_4$ is reported and compared to that of oxidized $NaAlH_4$, thus illustrating the power of XANES spectroscopy as a quick qualitative check of the $NaAlH_4$. For the EXAFS data, reliable fits of the Al K-edge spectra could be obtained when all scattering contributions, i.e., Al−H, Al−Na, and Al−Al, were incorporated into the fit. The hydrogen atoms made a significant contribution to the Al K-edge EXAFS signal of $NaAlH_4$, which stresses the importance of hydrogen scattering when analyzing EXAFS data of this metal hydride.

1. Introduction

To realize the application of sustainable energy schemes, storage of energy is essential. Hydrogen is regarded as a candidate to store energy for stationary and mobile applications. However, for the implementation of hydrogen technology in society, the challenge of hydrogen storage has to be addressed. Sodium alanate ($NaAlH_4$) is regarded as a promising hydrogen storage material because it has a high hydrogen capacity (5.6 wt %) and suitable thermodynamic stability for reversible hydrogen storage.[1,2] The hydrogen is released in two steps when $NaAlH_4$ is heated (eq 1), and hydrogen is reabsorbed by applying H_2 pressure.

$$NaAlH_4 \leftrightarrow {}^1/_3Na_3AlH_6 + {}^2/_3Al + H_2 \leftrightarrow NaH + Al + {}^3/_2H_2 \quad (1)$$

Unfortunately, the kinetics of hydrogen desorption and reloading of a desorbed alanate sample are unfavorable, with the latter most likely being a result of segregation of the NaH and Al phases.[3,4] We expect that the dynamics of the local structure around Al (and Na) can give insight into the mechanism of phase segregation, which will allow for the development of improved storage materials. To date, most structural properties of sodium alanate have been investigated with (synchrotron) X-ray diffraction,[5−7] neutron diffraction,[7,8] ^{1}H NMR spectroscopy, and ^{27}Al NMR spectroscopy.[9−11] The diffraction techniques require long-range ordering and, thus, do not provide information on the local environment around Al. In addition, NMR spectroscopy of solid materials is challenging to interpret. X-ray absorption spectroscopy, i.e., extended X-ray absorption fine structure (EXAFS) and X-ray absorption near-edge structure (XANES) spectroscopies, are suitable for determining local structures (EXAFS) and electronic/geometrical parameters (XANES) of a specimen and have been applied to determine the local structure of Ti in Ti-doped $NaAlH_4$ systems.[12−16] Recently, an Al K-edge XANES study on $NaAlH_4$ was reported.[17]

X-ray absorption measurements of low-*Z* elements, such as Na and Al, are challenging because of the low X-ray intensity of the synchrotron radiation in the required energy range (1000−2000 eV). Nevertheless, some successful studies on the Al K-edge have been performed on solid oxides and aluminum oxide gels[18−20] either in vacuum or in situ using a specially designed cell (ILEXAFS[21]). In contrast to aluminum oxides, measuring the XAFS spectrum of a metal hydride is experimentally challenging because of its sensitive nature toward oxygen, water, vacuum, and temperature. Therefore, sample handling before and during XAFS data collection require extra attention to obtain reliable data.

In this work, Al K-edge X-ray absorption spectra of $NaAlH_4$ were recorded in an ILEXAFS cell.[21] Because of the sensitivity of $NaAlH_4$ toward air and water, its XANES and EXAFS spectra are compared to those of an oxidized $NaAlH_4$ sample, and a discrepancy with recent XANES spectra reported by Fichtner et al.[17] is discussed. For EXAFS fitting, the significance of including aluminum−hydrogen scattering is discussed for $NaAlH_4$. No Al K-edge EXAFS study has been published before for $NaAlH_4$.

2. Experimental Section

2.1. Sample Preparations. All sample preparations were carried out in a nitrogen-filled glovebox equipped with a circulation purifier. Chemical operations were conducted using Schlenk techniques. The solvents [tetrahydrofuran (THF) and diethylether] were dried by distillation over Na. Commercially available $NaAlH_4$ (Sigma-Aldrich) was purified by dissolving it in an excess of THF; remaining solids were removed by filtration. Next, the THF was evaporated by vacuum until precipitation started. In the following step, the $NaAlH_4$ was further precipitated by dropwise addition of diethylether. The crystallinity of the obtained $NaAlH_4$ was checked by X-ray diffraction, and only the sharp diffractions of the $NaAlH_4$ were present (not shown). Part of this $NaAlH_4$ sample was exposed to ambient air for 2 days and is hereafter referred to as "oxidized $NaAlH_4$".

2.2. XAFS Recording. X-ray absorption spectroscopy was performed on the Al K-edge (1561.1 eV) using an ILEXAFS

* To whom correspondence should be addressed. E-mail: j.h.bitter@chem.uu.nl.
[†] Universiteit Utrecht.
[‡] CCLRC Daresbury Laboratory.

10.1021/jp068678+ CCC: $37.00
Published on Web 07/17/2007

TABLE 1: Input Parameters for FEFF to Create the Reference Files

	N	R (Å)	S_0^2	σ^2 (10^3 Å^{-2})	V_r (eV)	V_i (eV)	potential	ref
Al−Na	1	2.86	0.78	3.28	9.00	1.0	Hedin−Lunqvist	
Al−Al	1	2.86	0.78	3.28	9.00	1.0	Hedin−Lunqvist	25
Al−H	1	1.63	1.00	0	0	1.0	Hedin−Lunqvist	
Al−H	1	2.93	1.00	0	0	1.0	Hedin−Lunqvist	
Al−O	1	1.71	0.80	5.39	7.63	1.0	Hedin−Lunqvist	Zn−AlPO−34

cell[21] in fluorescence mode with a gas proportional detector. Measurements were conducted on station 3.4 at the SRS (Synchrotron Radiation Source, Daresbury, U.K.), which was equipped with a YB_{66} double-crystal monochromator. Higher harmonics were removed by increasing the incident angle for the plane premirror to 0.8° and using a dual carbon on silicon coating. The storage ring was operated at 2.0 GeV and a mean current of 130 mA. $NaAlH_4$ was diluted 1:2 on a volume basis with BN to prevent self-absorption and loaded into the cell in a glovebox. Afterward, the cell was closed and transferred to the beamline. All EXAFS spectra were recorded at room temperature in flowing He that was purified using O_2 and H_2O gas clean filters from Varian Inc.

2.3. EXAFS Data Handling. EXAFS data analysis was done using XDAP.[22] The pre-edge background was approximated by a Victoreen function before subtraction.[23] The edge energy was determined at the maximum of the first derivative of the spectrum and was calibrated to the edge energy of Al foil (1559.0 eV). The spectrum was corrected for the background with a cubic spline.[24] During the background extraction procedure, the atomic X-ray absorption fine structure (AXAFS) was removed from the data, by minimizing the intensity from 0 to 1 Å in R space without significantly reducing the intensity of the most intense peak.[25,26] Normalization was performed by dividing the absorption spectrum by the height of the background at 50 eV above the edge. Four spectra were averaged to improve the signal-to-noise ratio.

Phase shifts and backscattering amplitudes of the different absorber−backscatter pairs were calculated using the FEFF 8.0 code.[27] For Al−Al scattering in $NaAlH_4$, the reference was calculated using the input parameters as described by Rehr et al.[28] The input values for FEFF are listed in Table 1. For Al−Al and Al−Na, the same backscattering amplitude and phase-shift functions were used, which is allowed because Al and Na are next-nearest neighbors in the periodic table.[29] Because Na and Al have similar scattering properties and the distances and coordination numbers of the Na and Al in the fourth/fifth shell (3.74 Å) are the same (based on crystal structure), the refined parameters for both atoms were constrained to the same value. Because of the absence of literature to fit Al−H scattering in low-Z metal hydrides, the Al−H scattering phases and amplitude were calculated without additional entries in the FEFF input file, and the parameters are listed in Table 1. The Al−O scattering phase and amplitude of a single absorber backscatterer was calculated with the parameters listed in Table 1, ensuring that the fit of the first Al−O shell of the experimentally recorded Zn−AlPO−34 had $\Delta\sigma^2$ and E_0 values of 0, with four Al−O atoms at 1.71 Å.[30,31]

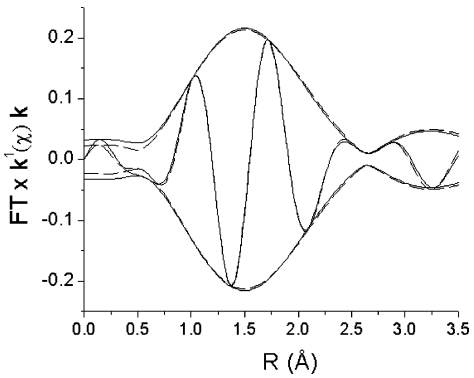

Figure 1. k^1 R-space fit of oxidized $NaAlH_4$ (• • •) (Δk, $3 < k < 7$ Å^{-1}; fit range, $0.5 < R < 3.5$ Å) and raw data (—) for an oxidized $NaAlH_4$ sample.

The Fourier transforms (FTs) of the EXAFS data were fitted using "the difference file technique" in R space,[25] using a k^0 weighting with a k range from 2.6 to 7 Å^{-1}. In all fits, the coordination numbers from crystallographic data were used as fixed input parameters.[5−8] R, ΔE_0, and $\Delta\sigma^2$ were refined to optimal values in the fitting process. The quality of the fit was checked by means of the k^0 variance and further checked by using k^0, k^1, and k^3 weightings of the difference files.[25]

3. Results and Discussion

3.1. Comparison of Oxidized and Nonoxidized $NaAlH_4$. Because $NaAlH_4$ is very reactive toward oxygen and water, XAFS results can be easily influenced by (partial) oxidation of the sample. Therefore, the XAFS analysis of an oxidized $NaAlH_4$ sample is discussed first. Oxidized $NaAlH_4$ was obtained by exposing $NaAlH_4$ to ambient air for 2 days. The EXAFS fit of the oxidized $NaAlH_4$ sample is shown in Figure 1. The fit parameters are listed in Table 2, and Al was surrounded with 5.9 oxygen atoms at 1.86 Å. The Al−O distance and coordination number correspond to a typical octahedral surrounding of Al in aluminum oxides/hydroxides in the ICSD crystallographic database and indicate that the sample was completely oxidized. In the next shell, 3.8 Al atoms were fitted at 3.00 Å. These data are not sufficient to conclude which aluminum−sodium oxide/hydroxide phase was formed.

The XANES spectra of octahedrally coordinated aluminum oxides/hydroxides display an intense sharp whiteline.[19,20] However, the here-reported whiteline of the oxidized $NaAlH_4$ sample was not as intense and sharp (Figure 2), whereas the Al−O environment in the EXAFS spectrum indicated an octahedral surrounding (Table 2). This is tentatively explained by the fact that the long-range structure around Al was very disordered, thereby reducing the intensity of the whiteline.[32]

Most noticeable in the XANES spectrum of oxidized $NaAlH_4$ are the two features on the whiteline at 1569.8 and 1571.3 eV. These features are absent in the spectrum of pure $NaAlH_4$. In addition, the edge position for oxidized alanate was located at 1565.6 eV, whereas for pure alanate, it was at 1561.1 eV

TABLE 2: Fit of Oxidized $NaAlH_4$[a]

absorber−backscatterer	N	$\Delta\sigma^2$ (10^3 Å^{-2})	R (Å)	ΔE_0 (eV)	k^0 variance: imaginary	k^0 variance: real
Al−O	5.9	1.31	1.86	−1.33	0.15	0.07
Al−Al	3.8	6.84	3.00	0.45		

[a] Number of free parameters was 8, and the maximum allowed number was 9.

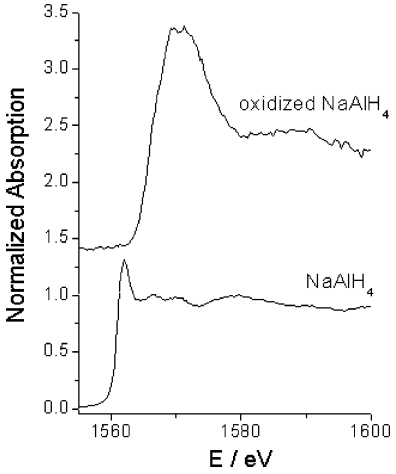

Figure 2. XANES spectra of $NaAlH_4$ and an oxidized $NaAlH_4$ sample. Spectra are normalized to 1580 eV.

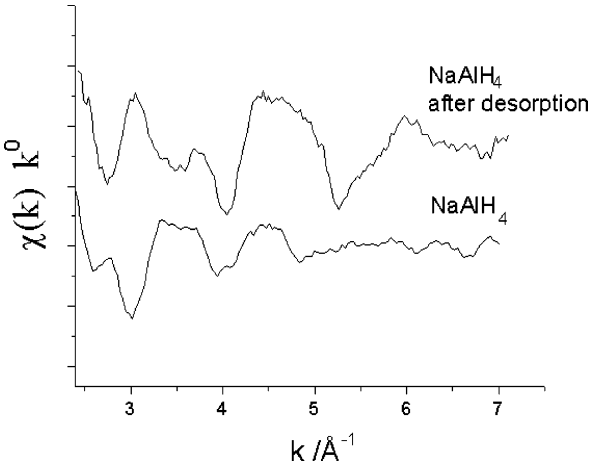

Figure 3. Background-subtracted EXAFS data for $NaAlH_4$.

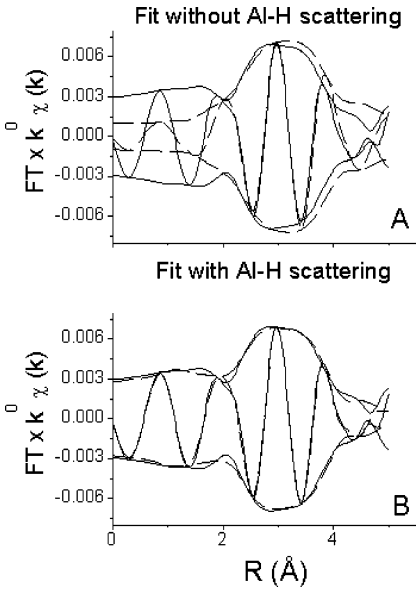

Figure 4. k^0 fits of $NaAlH_4$ (a) without hydrogen scattering (Δk, $2.6 < k < 7$ Å^{-1}; fit range, $0.5 < R < 4.5$ Å) and (b) with hydrogen scattering (Δk, $2.6 < k < 7$ Å^{-1}; fit range, $0.5 < R < 4.5$ Å). Raw data (—) and fit (− − −).

(Figure 2). Thus, the compounds can be easily distinguished using the XANES spectra as a fingerprint. Therefore, we must conclude that a recently published XANES spectrum of $NaAlH_4$ by Fichtner et al.,[17] which shows features identical to those of our air-exposed $NaAlH_4$ sample, was most likely a XANES spectrum not of $NaAlH_4$ but of oxidized $NaAlH_4$.

TABLE 3: Fit of $NaAlH_4$ without Hydrogen Scattering[a]

absorber−backscatterer	N	$\Delta\sigma^2$ (10^3 Å^{-2})	R (Å)	ΔE_0 (eV)	k^0 variance: imaginary	k^0 variance: real
Al−Na	4	6.4[b]	3.49[b]	−0.18[b]	2.17	9.58
Al−Na	4	12.3[b]	3.71[b]	3.46[b]		
Al−Al	4	12.3[c]	3.71[c]	3.46[c]		

[a] Number of free parameters was 6, and the maximum allowed number was 13. [b] Refined parameters. [c] Fitted with parameters identical to those used for the second Al−Na shell.

TABLE 4: Fit of $NaAlH_4$ with Hydrogen Scattering[a]

absorber−backscatterer	N	$\Delta\sigma^2$ (10^3 Å^{-2})	R (Å)	ΔE_0 (eV)	k^0 variance: imaginary	k^0 variance: real
Al−H	4	35[b]	1.63[b]	5.86[b]	0.20	0.22
Al−H	4	4.5[b]	2.95[b]	2.43[b]		
Al−Na	4	7.4[b]	3.53[b]	−2.92[b]		
Al−Na	4	11.7[b]	3.74[b]	1.65[b]		
Al−Al	4	11.7[c]	3.74[c]	1.65[c]		

[a] Number of free parameters was 12, and the maximum allowed number was 13. [b] Refined parameters. [c] Fitted with parameters identical to those used for the second Al−Na shell.

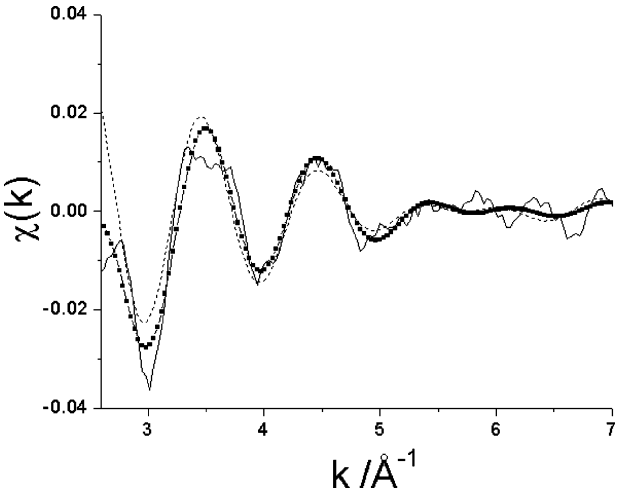

Figure 5. $\chi(k)$ of raw data (—): (−●−) fit with hydrogen scattering, (− − −) fit without hydrogen scattering.

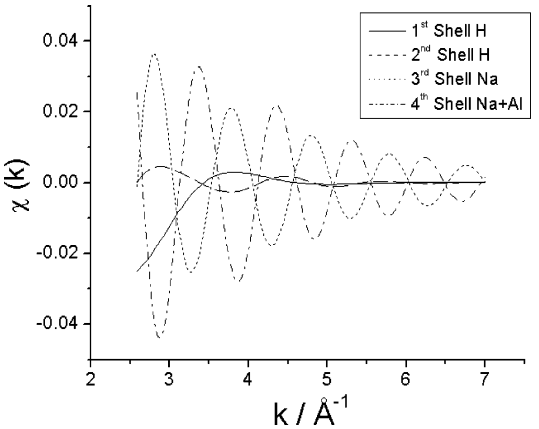

Figure 6. Calculated $\chi(k)$ values of the different atomic contributions to the total fit for $NaAlH_4$.

3.2. EXAFS Analysis of $NaAlH_4$. The background-subtracted EXAFS data of nonoxidized $NaAlH_4$ and the same $NaAlH_4$ sample after desorption are shown in Figure 3. Clearly, for

TABLE 5: Local Distances of $NaAlH_4$ Obtained from the Literature and from This Study

ref	technique	Al−H	Al−H	Al−Na	Al−Na	Al−Al
6	XRD	1.63	2.84	3.53	3.73	3.73
7	XRD and neutron diffraction	1.60	2.94	3.55	3.79	3.79
8	XRD and neutron diffraction	1.63	2.88	3.52	3.74	3.74
this study	EXAFS spectroscopy	1.63	2.95	3.53	3.74	3.74

$NaAlH_4$, the EXAFS spectrum was featureless at $k > 5.5$ Å^{-1}. To rule out the possibility that this is the result of an experimental limitation, the sample was heated to desorb hydrogen, thereby changing the local structure of Al. Figure 3 shows that, after the desorption of hydrogen, the EXAFS oscillations are visible up to $k = 7.0$ Å^{-1}. These results were reproducible when another $NaAlH_4$ sample was prepared and desorbed; thus, we concluded that the low intensity of the EXAFS oscillations for values of k higher than 5.5 Å^{-1} in the original sample are related to its structure. Note that the sample after desorption was included only for comparison; it will be discussed in detail elsewhere.

The data for $NaAlH_4$ were fitted using two different models. In the first model, only the Al−Al and Al−Na scattering was taken into account, and the data were fitted for $R = 0.5$−4.5 Å. The fit describing this model is displayed in Figure 4a with a dotted line and is referred to as the "fit without Al−H scattering". It can be seen that the FT of the fit strongly deviates from the FT of the data for $0 < R < 2$ Å. In addition, the fit also deviated slightly from the raw data for $2 < R < 4.5$ Å, i.e., where Na and Al scatterers are expected and fitted. In the second model, Al−H scattering was also included in the fit. The FT of the fit is shown in Figure 4b (dotted line) and describes the data adequately in the entire fitted range (0.5−4.5 Å).

The EXAFS coordination parameters are given in Table 3 for the fit without hydrogen scattering and in Table 4 for the fit with hydrogen scattering. The k^0 variances for the fit with hydrogen scattering (Table 4) were an order of magnitude lower than those for the fit without hydrogen scattering (Table 3); thus, the quality of the fit improved considerably when hydrogen was taken into account.

The raw data in k space are compared to the fits with and without hydrogen scattering in Figure 5. It can be seen that both fits describe the raw data at $k > 3.2$ Å^{-1}. However, including hydrogen into the fit improved the fit at low k values ($2.6 < k < 3.2$ Å^{-1}). This can be explained by the fact that the scattering power of the first hydrogen shell is strongest from 2.6 to 3.5 Å^{-1} in k space (Figure 6). For these reasons, it is important to extend the k range to a low value (e.g., 2.6 Å^{-1}) when the Al−H scattering is fitted. Extending the k range to a lower value has been reported before, ensuring that contributions of a light scatterer are not removed from the data.[33,34]

The calculated contributions of the individual scatterers to the Al K-edge EXAFS spectrum of $NaAlH_4$ are visualized in Figure 6. It is noted that the third (Al−Na) and fourth (Al−Na and Al−Al) shells are out of phase with each other, i.e., interfere destructively. This leads to a damped EXAFS signal for $NaAlH_4$ (Figure 3) when the coordination numbers are high.[26]

It is seen in Table 4 that the Debye−Waller factors ($\Delta\sigma^2$) for the hydrogen atoms were considerably higher than those for Al and Na, even when we take into account the fact that the Debye−Waller for Al−H was set to 0 in the reference file. This indicates that the position of the hydrogen atoms was more disordered than those of the Na and Al atoms, which is probably caused by increased thermal disorder, as a hydrogen atom is significantly lighter than a Na or Al atom.

Hydrogen scattering was previously directly detected in GdMg switchable mirrors,[35] in which the hydrogen was bonded to the Gd. Indirect hydrogen scattering was inferred from Pd−Pd lattice expansion using the lens effect in hydrides.[36] In water, hydrogen has been detected from the O K-edge EXAFS spectrum.[37]

A comparison between the structural parameters of $NaAlH_4$ from the literature and those from our EXAFS experiments is summarized in Table 5. The fitted distances for the hydrogen, sodium, and aluminum atoms in the EXAFS fit (Table 4) are in very good agreement with both the X-ray diffraction[6,7] and neutron diffraction studies,[7,8] thus illustrating the power of the approach.

Conclusions

The XANES spectrum of unoxidized $NaAlH_4$ has been recorded, and it was illustrated that the "fingerprint" of the XANES spectrum can be used as a quick quality control of the $NaAlH_4$ sample for, e.g., oxidation. The EXAFS spectrum of $NaAlH_4$ was measured and could be fitted according to the data on crystallographic distances. The EXAFS analysis shows that the inclusion of Al−H scattering is essential for the refinement. These findings indicate crucial issues that should be taken into account when analyzing the structural changes in X-ray absorption spectra occurring during the loading and unloading of metal hydrides.

Acknowledgment. This work was financially supported by ACTS, Project 053.61.02, and SRS Daresbury Laboratory, Project 43106. We thank Dr. Gopinathan Sankar from the Royal Institution of Great Britain for providing Zn−AlPO−34.

References and Notes

(1) Schlapbach, L.; Züttel, A. *Nature* **2001**, *414*, 353−358.
(2) Schüth, F.; Bogdanovic, B.; Felderhoff, M. *Chem. Commun.* **2004**, *20*, 2249−2258.
(3) Baldé, C. P.; Hereijgers, B. P. C.; Bitter, J. H.; de Jong, K. P. *Angew. Chem., Int. Ed.* **2006**, *45*, 3501−3503.
(4) Bodganovic, B.; Brand, R. A.; Marjanovic, A.; Schwickardi, M.; Tolle, J. *J. Alloys Compd.* **2000**, *302*, 36−58.
(5) Gross, K. J.; Guthrie, S.; Takara, S.; Thomas, G. *J. Alloys Compd.* **2000**, *297*, 270−281.
(6) Bel'skii, V. K.; Bulychev, B. M.; Golubeva, A. V. *Zh. Neorg. Khim.* **1983**, *28*, 2694−2696.
(7) Ozolins, V.; Majzoub, E. H.; Udovic, T. J. *J. Alloys Compd.* **2004**, *375* (1−2), 1−10.
(8) Hauback, B. C.; Brinks, H. W.; Jensen, C. M.; Murphy, K.; Maeland, A. J. *J. Alloys Compd.* **2003**, *358* (1−2), 142−145.
(9) Bogdanovic, B.; Felderhof, M.; Germann, M.; Pommerin, A.; Schueth, F.; Weidentaler, C.; Zibrowius, B. *J. Alloys Compd.* **2003**, *350*, 246−255.
(10) Majzoub, E. H.; Herberg, J. L.; Stumpf, R.; Spangler, S.; Maxwell, R. S. *J. Alloys Compd.* **2005**, *394* (1−2), 265−270.
(11) Majer, G.; Stanik, E.; Banuet, L. E. V.; Grinberg, F.; Kircher, O.; Fichtner, M. *J. Alloys Compd.* **2005**, *404*, 738−742.
(12) Felderhoff, M.; Klementiev, K.; Grünert, W.; Spliethoff, B.; Tesche, B.; Von Colbe, J. M. B.; Bogdanovic, B.; Hartel, M.; Pommerin, A.; Schüth, F.; Weidenthaler, C. *Phys. Chem. Chem. Phys.* **2004**, *6*, 4369−4374.
(13) Graetz, J.; Reilly, J. J.; Johnson, J.; Ignatov, A. Y.; Tyson, T. A. *Appl. Phys. Lett.* **2004**, *85* (3), 500−502.
(14) Léon, A.; Kircher, O.; Rothe, J.; Fichtner, M. *J. Phys. Chem. B* **2004**, *108* (42), 16372−16376.
(15) Léon, A.; Kircher, O.; Fichtner, M.; Rothe, J.; Schild, D. *J. Phys. Chem. B* **2006**, *110*, 1192−1200.

(16) Baldé, C. P.; Stil, H. A.; van der Eerden, A. M. J.; de Jong, K. P.; Bitter, J. H. *J. Phys. Chem. C* **2007**, *111*, 2797−2802.
(17) Léon, A.; Balerna, A.; Cinque, G.; Frommen, C.; Fichtner, M. *J. Phys. Chem. C* **2007**, *111* (9), 3796−3798.
(18) van Bokhoven, J. A.; Roelofs, J. C. A. A.; de Jong, K. P.; Koningsberger, D. C. *Chem. Eur. J.* **2001**, *7*, 1258−1265.
(19) van Bokhoven, J. A.; Sambe, H.; Ramaker, D. E.; Koningsberger, D. C. *J. Phys. Chem. B* **1999**, *103* (36), 7557−7564.
(20) Beale, A. M.; van der Eerden, A. M. J.; Grandjean, D.; Petukhov, A. V.; Smith, A. D.; Weckhuysen, B. M. *Chem. Commun.* **2006**, *42*, 4410−4412.
(21) van der Eerden, A. M. J.; van Bokhoven, J. A.; Smith, A. D.; Koningsberger, D. C. *Rev. Sci. Instrum.* **2000**, *71*, 3260.
(22) Vaarkamp, M.; Linders, J. C.; Koningsberger, D. C. *Physica B* **1995**, *208*/*209*, 159.
(23) Teo, B. K. *EXAFS: Basic Principals and Data Analysis*; Springer: New York, 1986.
(24) Cook, J. W., Jr.; Sayers, D. E. *J. Appl. Phys.* **1981**, *52*, 5024.
(25) Koningsberger, D. C.; Mojet, B. L.; Van Dorssen, G. E.; Ramaker, D. E. *Top. Catal.* **2000**, *10* (3−4), 143−155.
(26) Tromp, M.; van Bokhoven, J. A.; Arink, A. M.; Bitter, J. H.; Van Koten, G.; Koningsberger, D. C. *Chem. Eur. J.* **2002**, *8* (24), 5567−5678.
(27) Rehr, J. J.; Albers, R. C. *Rev. Mod. Phys.* **2000**, *72*, 621.
(28) Sikora, T.; Hug, G.; Jaouen, M.; Rehr, J. J. *Phys. Rev. B: Condens. Matter Mater. Phys.* **2000**, *62*, 1723−1732.
(29) Balzaroti, A.; De Crescenzi, M.; Incoccia, L. *Phys. Rev. B: Condens. Matter Mater. Phys.* **1982**, *25* (10), 6349−6365.
(30) Gonzales, G.; Pina, C.; Jacas, A.; Hernandez, M.; Leyva, Z. *Microporous Mesoporous Mater.* **1998**, *25*, 103−108.
(31) Ito, M.; Shimoyama, Y.; Saito, Y. *Acta Crystallogr.* **1985**, *C41*, 1698−1700.
(32) Gilbert, B.; Frazer, B. H.; Zhang, H.; Huang, F.; Banfield, J. F.; Haskel, D.; Lang, J. C.; Srajer, G.; De Stasio, G. *Phys. Rev. B: Condens. Matter Mater. Phys.* **2002**, *66*, 245205.
(33) Ramaker, D. E.; van Dorssen, G. E.; Mojet, B. L.; Koningsberger, D. C. *Top. Catal.* **2000**, *10*, 157−165.
(34) Zhang, Y.; Toebes, M. L.; van der Eerden, A. D.; O'Grady, W. E.; de Jong, K. P.; Koningsberger, D. C. *J. Phys. Chem. B* **2004**, *108*, 18509−18519.
(35) Di Vece, M.; Van der Eerden, A. M. J.; Van Bokhoven, J. A.; Lemaux, S.; Kelly, J. J.; Koningsberger, D. C. *Phys. Rev. B: Condens. Matter Mater. Phys.* **2003**, *67*, 035430.
(36) Lengeler, B. *Phys. Rev. Lett.* **1984**, *53*, 74.
(37) Wilson, K. R.; Tobin, J. G.; Ankudinov, A. L.; Rehr, J. J.; Saykally, R. J. *Phys. Rev. Lett.* **2000**, *85*, 4289.